Implicit numerical integration for the simulation and control of a non-smooth system with resets

Olivier Huber, Harshal Oza

Implicit numerical integration for the simulation and control of a non-smooth system with resets

Olivier Huber and Harshal B. Oza

***Abstract*— This paper presents a new method for numerical integration of a class of non-smooth systems in the presence of resets in position. The hard non-linearity introduced by resets due to a unilateral constraint on position poses a challenge for traditional numerical integration schemes which invariably result in oscillations. The results of this paper utilize the implicit numerical integration schemes of non-smooth systems to the systems with resets via employing the method of Zhuravlev-Ivanov transformation. The contribution lies in attaining existence of discretization solutions in the presence of the Zeno mode of impacts. We illustrate the effectiveness of the method on regulation and tracking problems. The good results presented here will motivate the theoretical study of those control strategies.**

***Index Terms*— implicit discretization, Zhuravlev-Ivanov transformation, twisting controller, variational inequalities**

I. Introduction

This paper deals with the numerical integration of non-smooth systems with resets. Resets are studied in various disciplines of engineering. For example, impacts due to collisions cause sudden jumps in velocity in mechanical systems. Study of biped robots poses itself nicely to the results in impact mechanical systems [1]. Another active research area within the control engineering community is that of hybrid systems where jumps represent the discrete events connecting the multiple continuous dynamics. Analytical proofs of stability of hybrid systems and numerical integration of trajectories are challenging to attain when an infinite number of events occur [2], [3].

Resets present hard non-linearities in the closed-loop system and often a destabilizing one for impact mechanical systems. It is well-known in the area of numerical integration of discontinuous systems that event-based explicit numerical schemes are inherently prone to spurious oscillations close to the discontinuity surface [4, Section 1.2.3.1]. Even for stable systems such as the bouncing ball, for example, it is difficult to "see through" the accumulation point in discrete-time and to achieve a numerically integrated solution that mimics the known continuous time counterpart closely.

The authors acknowledge the support of the ANR grant CHASLIM (ANR-11-BS03-0007). This material is based upon work supported by Air Force Grant FA9550-15-1-0212 and by the U.S. Department of Energy, Office of Science, Office of Advanced Scientific Computing Research, Applied Mathematics program under contract number DE-AC02-06CH11357 through the Project "Multifaceted Mathematics for Complex Energy Systems".

O. Huber is with the Wisconsin Institute for Discovery, University of Wisconsin-Madison, 330 N. Orchard St., Madison, WI, 53715, USA; H. Oza is with School of Engineering & Applied Science, Ahmedabad University, Gujarat, India. ohuber2@wisc.edu, harshal.oza@ahduni.edu.in

The main contribution of this paper lies in proposing simulation solution for a class of impact systems where such oscillations are not observed. Another motivation lies in the fact that numerical integration via the recently revived method of Zhuravlev [5] and Ivanov [6] non-smooth transformation offers a possibility to avoid impacts altogether. For a first look into this transformation, see the exposition in [10, Section 1.4.3].

The major difficulty with a unilaterally constrained mechanical system is the possible occurrence of the Zeno phenomenon. The latter is defined as the occurrence of an infinite number of events over a compact interval of time. In the case of a bouncing ball on the floor, if the ball loses energy at each impact, then it comes at rest in finite-time. With this simple model, the equilibrium is reached after the ball bounces an infinite number of times. This Zeno phenomenon is troublesome for the simulation of such systems. In particular, traditional event-driven schemes cannot numerically integrate the dynamics. Variants of this class of schemes have been developed to handle such system, see [4]. On the other hand, the time-stepping algorithm [7] is able to deal with such systems. However, the drawback is the low order of the method as against an event-driven scheme which can have a high-order in the free phase (when there is no impact). There has been some research efforts for studying these systems from a control perspective, including the design of controllers and observers [8], [9].

The proposed approach departs from these works by using the Zhuravlev-Ivanov transformation to work on an unconstrained dynamical system. Recent results regarding uniform finite time stability of a class of impact mechanical systems via non-smooth transformation can be found in [11] for a continuous time problem formulation. The paper considers mechanical systems with the Lagrangian dynamics recasted as a first-order system. A unilateral constraint is assumed to be present so that a jump in velocity is observed every time the constraint is active. Next, a desired trajectory of the system is expressed as a continuous dynamics with impacts. Then, the non-smooth state transformation is applied to transform both the desired and given plant dynamics into a variable-structure like system where there are no jumps. The dynamics for the tracking errors is then easily expressed and the numerical integration is performed with an implicit scheme.

The main contributions of the presented work are as follows. The numerical integration scheme via the transformation enables the user to deal successfully with accumulation point in discrete-time. This method can work both

for regulator and tracking problems for the class of systems shown. The later has never been attempted and hence it is a significant contribution. Simulation of hybrid systems, for example, can benefit from the presented work. The main weakness of the approach is that it works only when there is one constraint of co-dimension one.

In the next section the Zhuravlev-Ivanov transformation is revisited and an illustration is given by simulating the bouncing ball problem. Then, in Section III the regulator and tracking problems are described. The discrete-time implementation is the topic of Section IV and numerical simulation examples are given in Section V.

II. Zhuravlev-Ivanov transformation

Let us recall the Zhuravlev-Ivanov change of variables as described in [6]. Consider the following scalar second-order system with a unilateral constraint:

$$\begin{cases} \ddot{x} = f(t, x, \dot{x}) & x > 0 \text{ or } x = 0, \dot{x} > 0 \\ \ddot{x} = \max\{0, f\} & x = 0 \text{ and } \dot{x} = 0 \\ \dot{x}^+ = -e\dot{x}^- & x = 0 \text{ and } \dot{x} < 0. \end{cases} \tag{1}$$

The scalar $e \in (0, 1)$ is the coefficient of restitution when the system hits the constraints at $x = 0$. The vector field $f\colon \mathbb{R} \times \mathbb{R} \times \mathbb{R} \to \mathbb{R}$ is supposed to be continuous in all its arguments. Note that the classical bouncing ball example can be modelled as (1). The idea is to define a pair of variables (s, v) that are absolutely continuous. The simplest definition of those is as follows:

$$x = |s|, \quad \dot{x} = Rv\,\mathrm{sgn}(s),$$
$$R := 1 - \kappa\,\mathrm{sgn}(s)\,\mathrm{sgn}(v), \qquad \kappa := \frac{1-e}{1+e} \quad 0 < \kappa < 1.$$

Then, the dynamics of the s and v variables is given by

$$\begin{cases} \dot{s} = Rv \\ \dot{v} = R^{-1}\,\mathrm{sgn}(s) f(t, |s|, Rv\,\mathrm{sgn}(s)). \end{cases} \tag{2}$$

Remark 1. The dynamics are in (2) are invariant by a change of sign in both s and v. Also, the transformation is not a bijection, i.e., both (s, v) and $(-s, -v)$ gives the same value for $(x, \dot{x})$. This comes at no surprise since in the plane $(x, \dot{x})$, the trajectories are restricted to the half-space $x \geq 0$, whereas (s, v) evolves freely in $\mathbb{R}^2$.

Reference [6] provides details of the well-posedness of the system (2), which relies on Filippov's framework for differential equations with discontinuous right-hand side [12]. This means that the $\mathrm{sgn}(\,\cdot\,)$ must then be defined as a multivalued map.

Definition 1 (Multivalued signum function)**.** Let $x \in \mathbb{R}$. The multivalued signum function $\mathrm{sgn}\colon \mathbb{R} \rightrightarrows \mathbb{R}$ is defined as: $\mathrm{sgn}(x) = \{1\}$ if $x > 0, \{-1\}$ if $x < 0, [-1, 1]$ if $x = 0$. When $x \in \mathbb{R}^n$, the multivalued signum function $\mathrm{sgn}\colon \mathbb{R}^n \rightrightarrows \mathbb{R}^n$ is defined as: for all $j = 1, \ldots, n$, $(\mathrm{sgn}(x))_j := \mathrm{sgn}(x_j)$.

Let us illustrate how the transformed system (2) evolves as well as the original one (1). The classical bouncing ball example is considered with the following parameters: $m = 1\mathrm{kg}$, $g = 9.81\mathrm{Nm}^2/\mathrm{kg}^2$, $\kappa = 0.41$, $x_0 = 1\mathrm{m}$, $\dot{x}_0 = 6\mathrm{m/s}$.

The numerical integration is performed by an implicit scheme and is detailed in the next section. To the best of our knowledge, this is the first report of a systematic procedure to simulate such system. The state-space and time evolution of the pair (s, v) is depicted in Fig. 1 and 2, respectively. The first figure is reminiscent of the phase plot of the twisting algorithm [13] and the system converges to the origin as expected. The temporal evolution of variable is shown in Fig. 2. The Zeno phenomenon (accumulation of events) begins to occur at about 2.45s. Now, consider the value of the signum functions in Fig. 3. Each switch in the value of $\mathrm{sgn}(v)$ corresponds to an impact and a change in the sign of the velocity see [6], [11] for details.

Note that after the ball has lost all its energy and is laying on the ground, the expressions $\mathrm{sgn}(s) = 0$ and $\mathrm{sgn}(v) = 1$ hold true in discrete-time even though both s and v are zero. This is due to the fact that whenever the system is at the origin, with $\mathrm{sgn}(s) = 0$, the right-hand side of (2) is zero for any value of $\mathrm{sgn}(v)$. Then the system stays at rest for all values of $\mathrm{sgn}(v)$. Finally, the temporal evolution of the position and the velocity of the system in the original coordinates is depicted in Fig. 4. As expected the system

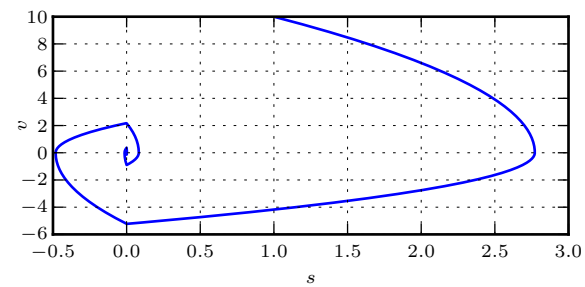

Fig. 1: Evolution of the transformed system in the (s, v) plane.

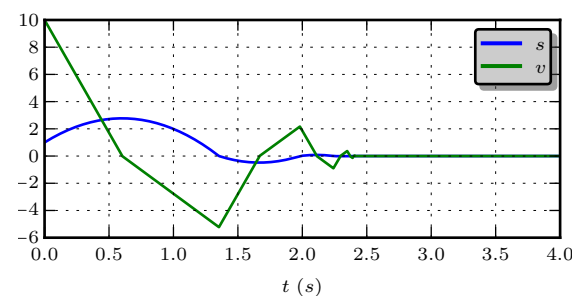

Fig. 2: Temporal evolution of the (s, v) variables.

bounces a few times and comes to a rest when all its energy has been lost due to the impacts.

III. Control strategies based on the Zhuravlev-Ivanov transformation

This section is dedicated to the control of system (1) when the dynamics are affine in control, that is

$$\ddot{x} = f(t, x, \dot{x}) + u(t).$$

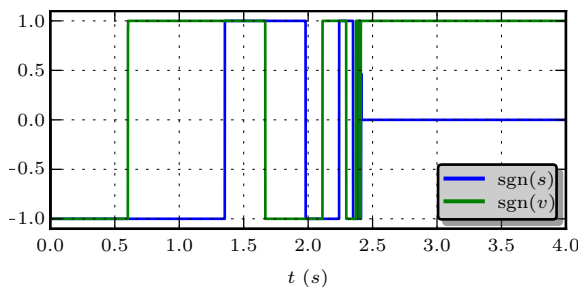

Fig. 3: Evolution of the signum variables.

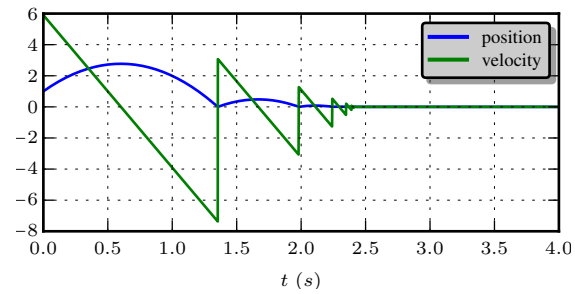

Fig. 4: Evolution of position and velocity of the ball.

A control law for the regulation problem has been proposed and studied in [11]. The closed-loop system has dynamics given by

$$\dot{s} = Rv \qquad R = 1 - \kappa \operatorname{sgn}(s) \operatorname{sgn}(v) \tag{3a}$$
$$\dot{v} = R^{-1} \operatorname{sgn}(s) F - R^{-1}(\mu_1 \operatorname{sgn}(s) + \mu_2 \operatorname{sgn}(v)), \tag{3b}$$

where F are the external forces acting on the system, bounded in magnitude by $M > 0$. This system is known to be globally finite-time stable whenever the gains are such that $M < \mu_2 < \mu_1 - M$.

The other control application is a tracking problem, where it is desired that the state of the system follows a reference trajectory. One peculiarity of the method is that the dynamics has to be specified in the (s, v) coordinates. The following control architecture is proposed: the controller computes the value of the control input via a one-step integration (between t_k and t_{k+1}) of the (s, v) system. The value of the control is then applied to the real system. The reference system is given by

$$\dot{s}_{\text{ref}} = R_{\text{ref}} v_{\text{ref}} \qquad R_{\text{ref}} = 1 - \kappa_{\text{ref}} \operatorname{sgn}(s_{\text{ref}}) \operatorname{sgn}(v_{\text{ref}}) \tag{4a}$$
$$\dot{v}_{\text{ref}} = R_{\text{ref}}^{-1} \operatorname{sgn}(s_{\text{ref}}) F_{\text{ref}}, \tag{4b}$$

with F_{ref} the desired external forces applied to the reference system. The controlled system in the (s, v) coordinates has dynamics given by

$$\dot{s} = Rv \qquad R = 1 - \kappa \operatorname{sgn}(s) \operatorname{sgn}(v) \tag{5a}$$
$$\dot{v} = R^{-1} \operatorname{sgn}(s)(u + F), \tag{5b}$$

with u the control input. The tracking errors in the transformed coordinates is defined as:

$$e_s = s - s_{\text{ref}} \quad \text{and} \quad e_v = v - v_{\text{ref}},$$

and its dynamics is

$$\dot{e}_s = Rv - R_{\text{ref}} v_{\text{ref}} \tag{6a}$$
$$\dot{e}_v = R^{-1} \operatorname{sgn}(s)(u + F) - R_{\text{ref}}^{-1} \operatorname{sgn}(s_{\text{ref}})(F_{\text{ref}}). \tag{6b}$$

Substituting R and R_{ref} in (6a) from (4a) and (5a) gives

$$\dot{e}_s = e_v - (\kappa \operatorname{sgn}(s)|v| - \kappa_{\text{ref}} \operatorname{sgn}(s_{\text{ref}})|v_{\text{ref}}|).$$

The control input is defined as

$$\begin{aligned} u = R \operatorname{sgn}(s) \big[& -\mu_1 \operatorname{sgn}(e_s) - \mu_2 \operatorname{sgn}(e_v) \\ & + R_{\text{ref}}^{-1} \operatorname{sgn}(s_{\text{ref}}) F_{\text{ref}} \big] - \operatorname{sgn}(s)^2 F. \end{aligned} \tag{7}$$

and is based on the twisting algorithm from second-order sliding mode control plus a correction term for the dynamics. Finally, the error dynamics is given by

$$\dot{e}_s = e_v - (\kappa \operatorname{sgn}(s)|v| - \kappa_{\text{ref}} \operatorname{sgn}(s_{\text{ref}})|v_{\text{ref}}|) \tag{8a}$$
$$\begin{aligned} \dot{e}_v = \operatorname{sgn}(s)^2 [& -\mu_1 \operatorname{sgn}(e_s) - \mu_2 \operatorname{sgn}(e_v) \\ & + R^{-1} \operatorname{sgn}(s)(1 - \operatorname{sgn}(s)^2) F] \\ & + (\operatorname{sgn}(s)^2 - 1) R_{\text{ref}}^{-1} \operatorname{sgn}(s_{\text{ref}}) F_{\text{ref}}. \end{aligned} \tag{8b}$$

Note that when $\operatorname{sgn}(s)^2 = 1$, the evolution of the error given in (8a)-(8b) is close to the twisting case, except for the second term in (8a). The solution of the above systems is to be understood in Filippov's framework and is absolutely continuous.

IV. Discrete-time controllers

This section gives details of the implicit numerical scheme. Since the control input is defined in the (s, v) space, all the computations are performed in those coordinates. At the time instant t_k, the knowledge of the pair $(x_k, \dot{x}_k)$ is available and they are needed to be transformed into (s_k, v_k). Remember from Remark 1 that both pairs (s, v) and $(-s, -v)$ gives the same value of $(x, \dot{x})$ and that the dynamics are also invariant under this change of sign. We choose to set $\operatorname{sgn}(s_k) = 1$. Then, $s_k = x_k$ and $v_k = \dot{x}_k/(1-\kappa)$. Then, the control u_k is computed as the result of a one-step integration of the (s, v)-dynamics. An alternative choice $\operatorname{sgn}(s_k) = -1$ would result in a similar analysis. It should be noted that in discrete-time the evolution of one time step is of interest and with the above choice in the transformed coordinates the trajectories will not jump.

A. Discretization of the dynamics

The discrete-time dynamics of the closed-loop system (8) is obtained with the $\theta - \gamma$ discretization method, see for instance [15]. Roughly speaking, it is an extension of the θ-method for the discretization of ordinary differential equations. The coefficient θ is used for the smooth part (the state) and γ for the nonsmooth component (the signums) of the ODE. The implicit discretization, a special case when $\theta = \gamma = 1$, has been used to successfully discretize discontinuous systems from mechanics (system with impact and friction [4]) and control theory (sliding mode control [16], [17]). To make the presentation more accessible, we focus on the implicit case. Let x^k be the value of the variable x at the

time t^k and x^{k+1} be the value at t^{k+1}. With the multivalued signum function, we have the following inclusions

$$\lambda_s^{k+1} \in \operatorname{sgn}(s^{k+1}) \qquad \lambda_v^{k+1} \in \operatorname{sgn}(v^{k+1}) \tag{9}$$
$$\lambda_{s_{\text{ref}}}^{k+1} \in \operatorname{sgn}(s_{\text{ref}}^{k+1}) \qquad \lambda_{v_{\text{ref}}}^{k+1} \in \operatorname{sgn}(v_{\text{ref}}^{k+1}) \tag{10}$$
$$\lambda_{e_s}^{k+1} \in \operatorname{sgn}(e_s^{k+1}) \qquad \lambda_{e_v}^{k+1} \in \operatorname{sgn}(e_v^{k+1}) \tag{11}$$
$$R_{\text{ref}}^{k+1} = 1 - \kappa_{\text{ref}} \lambda_{s_{\text{ref}}}^{k+1} \lambda_{v_{\text{ref}}}^{k+1} \qquad R^{k+1} = 1 - \kappa \lambda_s^{k+1} \lambda_v^{k+1}.$$

Note that since κ and κ_{ref} take value in $(0,1)$, both R_{ref}^{k+1} and R^{k+1} admit reciprocal. For the closed-loop system (3) (regulator case), the discrete-time dynamics is given by

$$s^{k+1} = R^{k+1} v^{k+1} \tag{12}$$
$$v^{k+1} = (R^{k+1})^{-1}(\lambda_s^{k+1} F^{k+1} - \mu_1 \lambda_s^{k+1} - \mu_2 \lambda_v^{k+1}) \tag{13}$$

Moving on to the tracking case, from (8), the discrete-time error dynamics is given by

$$\begin{aligned} h^{-1}(e_s^{k+1} - e_s^k) &= e_v^{k+1} + (R^{k+1} - 1) v^{k+1} \\ &\quad - (R_{\text{ref}}^{k+1} - 1) v_{\text{ref}}^{k+1} \end{aligned} \tag{14}$$
$$\begin{aligned} h^{-1}(e_v^{k+1} - e_v^k) &= (\lambda_s^{k+1})^2 [-\mu_1 \lambda_{e_s}^{k+1} - \mu_2 \lambda_{e_v}^{k+1} \\ &\quad + R^{k+1} \lambda_s^{k+1} (1 - (\lambda_s^{k+1})^2) F^{k+1}] \\ &\quad + ((\lambda_s^{k+1})^2 - 1)(R_{\text{ref}}^{k+1})^{-1} \lambda_{s_{\text{ref}}} F_{\text{ref}}^{k+1}. \end{aligned} \tag{15}$$

Note that the right-hand side of the evolution in e_s requires us to also integrate both the original and the reference systems. The dynamics of the original system is:

$$h^{-1}(s^{k+1} - s^k) = R^{k+1} v^{k+1} \tag{16}$$
$$\begin{aligned} h^{-1}(v^{k+1} - v^k) &= (\lambda_s^{k+1})^2 (-\mu_1 \lambda_{e_s}^{k+1} - \mu_2 \lambda_{e_v}^{k+1} \\ &\quad + (R_{\text{ref}}^{k+1})^{-1} \lambda_{s_{\text{ref}}}^{k+1} F_{\text{ref}}^{k+1}) \\ &\quad + R^{k+1} \lambda_s^{k+1} (1 - (\lambda_s^{k+1})^2) F^{k+1}, \end{aligned} \tag{17}$$

and for the reference system the following holds true:

$$h^{-1}(s_{\text{ref}}^{k+1} - s_{\text{ref}}^k) = R_{\text{ref}}^{k+1} v_{\text{ref}}^{k+1} \tag{18}$$
$$h^{-1}(v_{\text{ref}}^{k+1} - v_{\text{ref}}^k) = (R_{\text{ref}}^{k+1})^{-1} \lambda_{s_{\text{ref}}}^{k+1} F_{\text{ref}}^{k+1}. \tag{19}$$

Note that the dynamics of the reference system (18)-(19) is independent of the other ones, but this is not the case for (16)-(17) and (14)-(15). From (7), the discrete-time control input is defined as

$$\begin{aligned} u_k &= (R^{k+1})^{-1} \lambda_s^{k+1} \big[-\mu_1 \lambda_{e_s}^{k+1} - \mu_2 \lambda_{e_v}^{k+1} \\ &\quad + (R_{\text{ref}}^{k+1})^{-1} \lambda_{s_{\text{ref}}}^{k+1} F_{\text{ref}}^{k+1} \big] - (\lambda_s^{k+1})^2 F^{k+1}. \end{aligned} \tag{20}$$

Therefore, to compute the control input u_k, all three systems must be integrated. That is all unknowns in Equations (14) to (19) must be found simultaneously. There are 12 unknowns in those 6 equations . Also, the closed-loop dynamics (12)-(13) features 2 equations for 4 unknowns. At first, it appears that the computation is in jeopardy. However, let us show that the inclusion relations given in (9)-(10) can be used to remove all unknown states from the equations. Then the only unknowns are the signum values. This is achieved by combining the inclusions and equations into a variational inequality (VI).

B. VI reformulation

Basic convex analysis [18] tools are used to model the system of Equations (14) to (19) into a form amenable to computations. The main observation to perform the transformation into a VI is that any relation of the type $\lambda \in \operatorname{sgn}(s)$ (all scripts dropped for clarity) in Equations (9)-(11) can be rewritten as $\lambda \in \partial\sigma_{[-1,1]}(s)$, with $\sigma_K(x) := \sup_{y \in K} \langle y, x \rangle$ is the support function of the set K. Let us explain here the different objects. It can be readily check that

$$|x| = \sup_{y \in [-1,1]} \langle y, x \rangle = \sigma_{[-1,1]}(x). \tag{21}$$

Note that the element of $[-1,1]$ that realize the supremum is either 1 or x is positive, -1 if x is negative, or any element of $[-1,1]$ if $x = 0$. This is precisely the value of $\lambda \in \operatorname{sgn}(x)$, when sgn is given by Definition 1. Finally, the multivalued function $\partial\sigma \colon \mathbb{R} \rightrightarrows \mathbb{R}$ denotes the subdifferential of the support function: g is an element of $\partial\sigma_{[-1,1]}(x)$ if it realizes the supremum in (21). The following result holds by Fenchel duality:

$$\lambda \in \operatorname{sgn}(s) \iff s \in N_{[-1,1]}(\lambda), \tag{22}$$

where $N_K(\,\cdot\,) \colon \mathbb{R}^n \rightrightarrows \mathbb{R}^n$ is the normal cone operator defined as follows: $N_K(x) = \{\, d \in \mathbb{R}^n \mid \langle d, y - x \rangle \leq 0 \ \forall y \in K \}$. Using relation (22) in Equations (12) and (13), we get

$$\begin{aligned} 0 \in &\begin{pmatrix} -(R^{k+1} v_k + \lambda_s^{k+1} F^{k+1} - \mu_1 \lambda_s^{k+1} - \mu_2 \lambda_v^{k+1} \\ -(R^{k+1})^{-1}(\lambda_s^{k+1} F^{k+1} - \mu_1 \lambda_s^{k+1} - \mu_2 \lambda_v^{k+1}) \end{pmatrix} \\ &+ N_{[-1,1]^2} \begin{pmatrix} \lambda_s^{k+1} \\ \lambda_v^{k+1} \end{pmatrix}. \end{aligned} \tag{23}$$

Note that this generalized equation has only two unknowns: λ_s^{k+1} and λ_v^{k+1}. The same procedure enables us to transform Equations (14) to (19) into generalized equations featuring only 6 unknowns.

$$0 \in G_k(\Lambda) + N_{\mathcal{B}_\infty^6}(\Lambda), \tag{24}$$

where Λ collects all the signums and $\mathcal{B}_\infty^6$ is the unit ball for the infinite norm in $\mathbb{R}^6$, also written $[-1,1]^6$. The expression for G_k is given in the appendix. This function is indexed by k to denote that it changes at each time instant t_k. The inclusions (23) and (24) can be characterized even further by recognizing that it is an equivalent form of a Variational Inequality (VI). For instance, solving the VI associated with (24) consists in finding $\Lambda \in \mathcal{B}_\infty^6$ such that for all $w \in \mathcal{B}_\infty^6$,

$$(w - \Lambda)^T G_k(\Lambda) \geq 0.$$

This is easy to check from the definition of the normal cone operator.

Finite dimensional variational inequalities have been studied since the 70s and there is a nice body of literature devoted to their studies. The reader is referred to [19] for the most recent reference. Also, numerous algorithms have been developed to solve VIs. In the following, those tools are used to characterize the proposed controller and the control input is computed thanks to an algorithm for solving VI. First the well-posedness of the controller is considered.

Lemma 1. *The VIs* (23) *and* (24) *have always a solution.*

Proof. This result is well known as a special case (Corollary 2.2.5, p. 148 in [19]). □

Recall that the discrete-time control input (20) is the image by a continuous function of the solution Λ of the VI (24)

Corollary 1. *The controller with control input defined by* (20) *is non-anticipative.*

Proof. At time t_k, the map G_k is well defined and Lemma 1 give us the existence of a solution Λ to (24). Since the control law is a given by a continuous function of this solution Λ, the control input value is computable based on the information given at time t_k. □

V. Numerical experimentations

A. Approaches to solve VIs

For the computation of the control law, we use the PATH solver [21], via the SICONOS software package [22][1]. The procedure to solve a VIs like (23) and (24) is to successively solve Affine Variational Inequalities (AVI) via a pivotal procedure. Since we are dealing with box constraints, a variant of the Lemke algorithm is used. Since the set is compact, each AVI is processable [23, p. 55], that is the algorithm finds a solution to each subproblem. The check for the processability of the problem, that is finding a solution to the VI, is outside the scope of the paper.

When dealing with nonlinear problem as (23) or (24), there are two approaches to compute a solution.

- An outer linearisation, where the simulation software linearises the problem and task the optimization solver with finding a solution to an affine problem. To promote convergence, the problem is linearised until either a convergence criterion is met, or the maximum number of iterations is reached.
- An inner linearisation, where the optimization solver is tasked with solving the nonlinear problem directly. It relies on the simulation software to linearise the problem.

We strongly advise against using the first method to simulate such system since the solution of the linearised system may be of poor quality with respect to the nonlinear one. A solver like PATH uses a mechanism to retain the best point it finds during the solution of the linear system. The quality of the point is evaluated using a merit function, which is similar to a Lyapunov function but for an optimization algorithm. Therefore, the optimization solver can take advantage of information that is otherwise lost if it is the simulation software that performs the linearisation. In our experiments, the first method could not reliably find a solution in a large number of instances.

[1] http://siconos.gforge.inria.fr

B. Simulation results

First the result from a simulation of the system (3) is given in Fig. 5, with no external forces applied. The trajectory is like the one given by the twisting algorithm, which is expected. The next example illustrates the performance

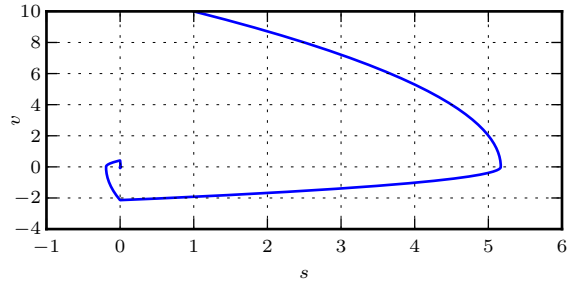

Fig. 5: Evolution of the pair (s, v) for the system (3).

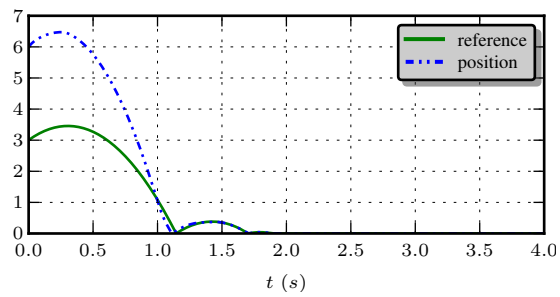

Fig. 6: Evolution of the positions of the two systems.

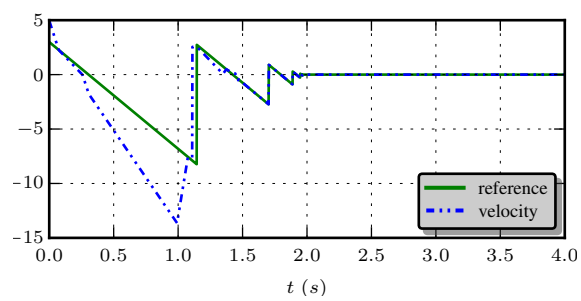

Fig. 7: Evolution of the velocities of the two systems.

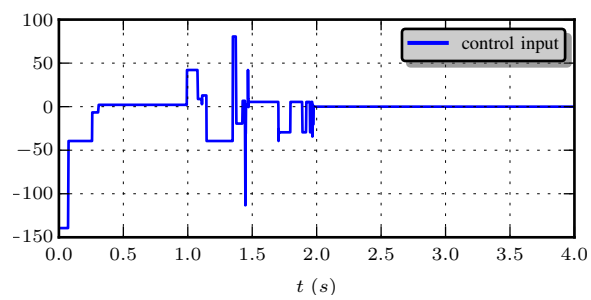

Fig. 8: Evolution of the control input value.

of the tracking controller (7) acting on (5), with identical coefficients of restitution. The setup is the following: $\mu_1 = 30$, $\mu_2 = 17$, $\kappa = \kappa_{\text{ref}} = 0.5$. The difference between the two systems are now given: first the initial state are $x^0 = 6, \dot{x}^0 = 5$ versus $x^0_{\text{ref}} = 3$ and $\dot{x}^0_{\text{ref}} = 3$. Then for the real system, the external forces is the classical gravity $F = -9.81$ SI

whereas for the reference, $F_{\rm ref} = -19.81$ SI. On Fig. 6, the positions of the two systems are given. The tracking takes place rapidly, and the controlled system undergoes the accumulation without any (numerical) difficulty. Velocities are given on Fig. 7 and the tracking also takes place quickly. Note that the twisting algorithm exhibits an overshooting behavior, before settling down. However, the tracking near the Zeno phenomenon is flawless. The corresponding control input is given on Fig. 8.

VI. Conclusion

The results presented in this paper give an implicit numerical integration scheme for tracking control problem for non-smooth systems with resets. The original problem of resets in the dynamics is first converted into a jump-free system via a non-smooth transformation. Then, the numerical integration of the non-smooth system is shown to be well-defined thanks to a reformulation as a VI. Such a method has a contribution in the simulation of hybrid systems of the class of constrained systems considered in the paper. Characterizing the stability of the closed-loop systems is part of the current research effort.

Acknowledgment

The authors thank Dr. Vincent Acary for discussions about the discretization of nonsmooth systems. The second author thanks Dr. Bernard Brogliato, Dr. Yury Orlov and Dr. Sarah Spurgeon for their support for the visit to INRIA Grenoble Rhône-Alpes and discussions for this work.

References

[1] C. Chevallereau, G. Abba, Y. Aoustin, F. Plestan, E. R. Westervelt, C. Canudas-de Wit, and J. W. Grizzle, "RABBIT: A testbed for advanced control theory," *Control Systems Magazine, IEEE*, vol. 23, no. 5, pp. 57–79, 2003.

[2] K. H. Johansson, M. Egerstedt, J. Lygeros, and S. Sastry, "On the regularization of Zeno hybrid automata," *Systems & Control Letters*, vol. 38, no. 3, pp. 141–150, 1999.

[3] M. D. O'Toole and E. M. Navarro-López, "A hybrid automaton for a class of multi-contact rigid-body systems with friction and impacts," in *4th IFAC Conference on Analysis and Design of Hybrid Systems*, 2012, pp. 299 – 306.

[4] V. Acary and B. Brogliato, *Numerical Methods for Nonsmooth Dynamical Systems: Applications in Mechanics and Electronics*, Lecture Notes in Applied and Computational Mechanics. Springer Berlin Heidelberg, 2008, vol. 35.

[5] V. F. Zhuravlev, "Equations of motion of mechanical systems with ideal one-sided links," *Journal of Applied Mathematics and Mechanics*, vol. 42, no. 5, pp. 781–788, 1978.

[6] A. P. Ivanov, "Analytical methods in the theory of vibro-impact systems," *Journal of Applied Mathematics and Mechanics*, vol. 57, no. 2, pp. 221–236, 1993.

[7] J. J. Moreau, "Unilateral contact and dry friction in finite freedom dynamics," in *Nonsmooth Mechanics and Applications*, International Center for Mechanical Sciences. Springer, 1988, vol. 302, pp. 1–82.

[8] A. Tanwani, B. Brogliato, and C. Prieur, "Observer design for unilaterally constrained Lagrangian systems: A passivity-based approach," *Automatic Control, IEEE Transactions on*, in press 2016.

[9] F. Forni, A. R. Teel, and L. Zaccarian, "Follow the bouncing ball: Global results on tracking and state estimation with impacts," *Automatic Control, IEEE Trans. on*, vol. 58, no. 6, pp. 1470–1485, 2013.

[10] B. Brogliato, *Nonsmooth Mechanics: Models, Dynamics and Control*, Communications and Control Engineering. Springer London, 1999.

[11] H. B. Oza, Y. V. Orlov, and S. K. Spurgeon, "Finite time stabilization of a perturbed double integrator with unilateral constraints," *Mathematics and Computers in Simulation*, vol. 95, pp. 200–212, 2014.

[12] A. F. Filippov, *Differential Equations with Discontinuous Righthand Sides*, Mathematics and Its Applications. Dordrecht: Kluwer Academic Publishers, 1988, vol. 18.

[13] A. Levant, "Sliding order and sliding accuracy in sliding mode control," *Int. Journal of Control*, vol. 58, no. 6, pp. 1247–1263, 1993.

[14] Y. Orlov, "Finite time stability and robust control synthesis of uncertain switched systems," *SIAM Journal on Control and Optimization*, vol. 43, no. 4, pp. 1253–1271, 2005.

[15] S. Greenhalgh, V. Acary, and B. Brogliato, "On preserving dissipativity properties of linear complementarity dynamical systems with the θ-method," *Numerische Mathematik*, vol. 125, no. 4, pp. 601–637, 2013.

[16] O. Huber, V. Acary, and B. Brogliato, "Lyapunov stability and performance analysis of the implicit discrete sliding mode control," *Automatic Control, IEEE Transactions on*, in press 2016.

[17] O. Huber, V. Acary, B. Brogliato, and F. Plestan, "Implicit discrete-time twisting controller without numerical chattering: Analysis and experimental results," *Contr. Eng. Pract.*, vol. 46, pp. 129–141, 2016.

[18] R. T. Rockafellar, *Convex Analysis*. Princeton University Press, 1997.

[19] F. Facchinei and J.-S. Pang, *Finite-Dimensional Variational Inequalities and Complementarity Problems, Volume I*, Springer Series in Operations Research. Springer-Verlag New-York, 2003.

[20] R. T. Rockafellar and R. J.-B. Wets, *Variational Analysis*, Grundlehren der mathematischen Wissenschaften. Springer Berlin Heidelberg, 2009, vol. 317.

[21] S. P. Dirkse and M. C. Ferris, "The PATH solver: a nommonotone stabilization scheme for mixed complementarity problems," *Optimization Methods and Software*, vol. 5, no. 2, pp. 123–156, 1995.

[22] V. Acary, M. Brémond, O. Huber, and F. Pérignon, "An introduction to Siconos," INRIA, Rapport Technique RT-0340, 2016. [Online]. Available: http://hal.inria.fr/inria-00162911

[23] M. Cao and M. C. Ferris, "A pivotal method for affine variational inequalities," *Mathematics of Operations Research*, vol. 21, no. 1, pp. 44–64, February 1996.

Appendix
Closed-loop formula for G_k

First note that the relations for the v variables as given in (15), (17), and (19) are already in the right form. It remains to inject the expressions of those variables at t_{k+1} into the one for the s variables. Let us start with the real system: from (17) we have

$$\begin{aligned} v^{k+1} = v^k + h\big[(\lambda_s^{k+1})^2(-\mu_1\lambda_{e_s}^{k+1} - \mu_2\lambda_{e_v}^{k+1} \\ +(R_{\rm ref}^{k+1})^{-1}\lambda_{s_{\rm ref}}^{k+1} + R^{k+1}\lambda_s^{k+1}(1-(\lambda_s^{k+1})^2)F^{k+1})\big] \end{aligned} \tag{25}$$

Using this expression in (16) yields

$$\begin{aligned} s^{k+1} = s^k + hR^{k+1}(v^k + h\big[(\lambda_s^{k+1})^2(-\mu_1\lambda_{e_s}^{k+1} \\ -\mu_2\lambda_{e_v}^{k+1} + (R_{\rm ref}^{k+1})^{-1}\lambda_{s_{\rm ref}}^{k+1}F_{\rm ref}^{k+1} \\ +R^{k+1}\lambda_s^{k+1}(1-(\lambda_s^{k+1})^2)F^{k+1})\big]. \end{aligned} \tag{26}$$

For the reference system, we have a similar formula:

$$v_{\rm ref}^{k+1} = v_{\rm ref}^k + h(R_{\rm ref}^{k+1})^{-1}\lambda_{s_{\rm ref}}^{k+1}F_{\rm ref}^{k+1} \tag{27}$$

$$s_{\rm ref}^{k+1} = s_{\rm ref}^k + hR_{\rm ref}^{k+1}v_{\rm ref}^k + h^2\lambda_{s_{\rm ref}}^{k+1}F_{\rm ref}^{k+1}. \tag{28}$$

Finally the error dynamics is given by

$$e_v^{k+1} = v^{k+1} - v_{\rm ref}^{k+1} \qquad e_s^{k+1} = s^{k+1} - s_{\rm ref}^{k+1}. \tag{29}$$

The function G_k is then given component-wise by the negative of the right-hand side of (25), (26), (27), (28), and (29). One can check that those contain only terms known at t_k or components of the unknown Λ. Also, continuity and differentiability on a (small) open superset of $\mathcal{B}_\infty^6$ are readily checked since each component is the composition of elementary functions enjoying those properties.